acoustics

Communication

From Spherical Harmonics to Gaussian Beampatterns

Kevin J. Parker [1,*] and Miguel A. Alonso [2]

[1] Department of Electrical and Computer Engineering University of Rochester, Rochester, NY 14627, USA
[2] Institute of Optics, University of Rochester, Rochester, NY 14627, USA; miguel.alonso@rochester.edu
* Correspondence: kevin.parker@rochester.edu

Abstract: The use of multipoles, otherwise called spherical wavefunctions, has been explored for acoustic fields that can be omnidirectional, for example, in scattering theory. Less developed is the use of spherical harmonic multipoles for the construction of directed beams, such as the Gaussian unfocused beampattern, which is an important reference beam in many practical applications. We develop the straightforward construction of a Gaussian unfocused beam using the special properties of the sum of spherical harmonics; these include the use of an imaginary offset in directing the forward propagation to the desired beampattern. Examples are given for narrowband and broadband pulse propagation in the ultrasound MHz range, with comparisons against a classical acoustics formulation of the Gaussian beam. The use of spherical harmonics forms an alternative framework for devising beampatterns, with apodization and concentration issues of the beam linked to an array of a limited number of discrete multipoles at the source.

Keywords: ultrasound; beampatterns; spherical harmonics; monopoles; Gaussian

check for updates

Academic Editors: Jian Kang and Michel Darmon

Received: 23 January 2025
Revised: 6 March 2025
Accepted: 7 March 2025
Published: 11 March 2025

Citation: Parker, K.J.; Alonso, M.A. From Spherical Harmonics to Gaussian Beampatterns. *Acoustics* **2025**, *7*, 14. https://doi.org/10.3390/acoustics7010014

1. Introduction

The Gaussian beam is an important practical and theoretical benchmark in acoustics, optics, and electromagnetic wave propagations [1]. The Gaussian function itself is special as an eigenfunction of the Fourier transform, jointly having the absolute minimum spread (or uncertainty) in both domains, with no sidelobes [2,3]. A number of papers by Breazeale and associates describe straightforward implementation approaches with analytic expressions for the beampatterns produced by an acoustic piston source with Gaussian apodization [4,5]. There are several reasons to consider the usefulness of multipole expansions that can be configured to produce a useful Gaussian beam in acoustics and optics. It has been shown that a range of general beampatterns and scattering patterns are well described by the superposition of spherical Bessel and spherical harmonic functions [6–8]. The particular case of the Gaussian beampattern is treated in Section 4.10.2 of the paper by Alonso and Moore [9] with multipole expansions. It also includes the use of an imaginary offset of the source locations, a scheme originally suggested by Kravtsov [10] and Deschamps [11] as a means of creating a more directional wave distribution. The imaginary source offset has also been applied to scalar Gaussian configurations [12], reflections, and the method of images that produce Gaussian electromagnetic beams [13,14]. More recently, the multipole framework for beampatterns was reconsidered in light of the special interpolation and localization properties of sums of spherical Bessel functions and spherical harmonic functions that form the free-space solution to the Helmholtz wave equation [15]. This framework enables the recasting of important beamforming topics, including apodization, focusing, and the axial and lateral intensity profiles in terms of the special properties of the spherical functions. However, it is not obvious that the sums of the spherical functions can be formulated into a classical Gaussian beampattern. We demonstrate that this can be realized in several ways, based on the unique properties of the spherical functions. Simulations were conducted using a 5 MHz ultrasound beam as an example.

2. Theory

The free-space solution to the Helmholtz equation for monochromatic waves in spherical coordinates is configured within a source cone of angle θ_s, as depicted in Figure 1.

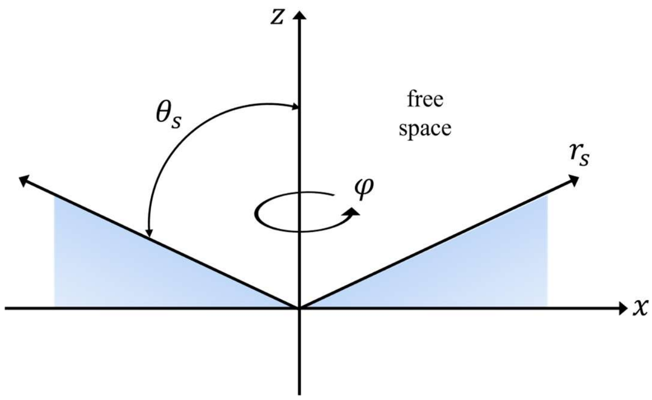

Figure 1. Definition of the spherical coordinate system (r, θ, φ) along with Cartesian coordinates (x, z). The active sources are, in general, located on the upper surface of the cone of angle θ_s; however, for the conventional unfocused Gaussian beam, we examine the case where this is coincident with the x axis to form a flat planar source.

The solution, limited to radially symmetric beampatterns and functions that are finite at $r = 0$, is given by

$$A(r, \theta) = \sum_{n=0}^{N} a_n j_n(kr) Y_n^0(\theta), \tag{1}$$

where r, θ, and φ are spherical coordinates, A is the scalar wave in free space with wavenumber k, a_n denotes the weights, j_n denotes the spherical Bessel functions, and Y_n^0 denotes the spherical harmonic functions with rotational symmetry [16]. Some of the special properties of these functions and their sums are as follows:

$$j_n(x) \to \sin\left(x - \frac{1}{2}n\pi\right)/x \text{ for } x \to \infty \tag{2}$$

$$\sum_{n=0}^{N} j_n(x) \cong \begin{cases} \dfrac{\sqrt{\pi/2}}{\sqrt{x}} & 0 < x \leq N \\ 0 & x > N \end{cases} \tag{3}$$

$$\sum_{n=0}^{N} \sqrt{(n + 1/2)} j_n(x) \cong \begin{cases} \sqrt{\pi/2} & 0 < x \leq N \\ 0 & x > N \end{cases} \tag{4}$$

$$\sum_{n=0}^{N} f(n)\left(\sqrt{(n + 1/2)} j_n(x)\right) \cong \begin{cases} (\sqrt{\pi/2}) f(x) & 0 < x \leq N \\ 0 & x > N \end{cases} \tag{5}$$

where n is an integer, and $f(x)$ is a well-behaved bandlimited function with discrete samples $f(n)$. Generally, these relationships are compatible with the classical series of functions, such as Neumann's expansion, the Fourier–Bessel series [16,17], and others found by Stevenson [18], Watson [19], and Erdélyi et al. [20]. These relationships can also be considered, from the point of view of signal processing, as interpolation functions analogous to the use of the "sinc" function (which is identical to the j_0 function) for the interpolation of sampled signals. For example, Equation (5) can be interpreted as a reconstruction of some well-behaved continuous function $f(x)$ from discrete samples $f(n)$. The approximation signs are used in Equations (3)–(5) due to the small oscillations or ripples associated with band-limited interpolation. Furthermore, and importantly, Equation (1) can be considered a design specification, for if we generate a particular spherical harmonic pattern as an active source at the surface of the cone of Figure 1, the resulting free-field solution will be constructed in the interior. For flat pistons, theta at the source plane is simply $\pi/2$.

Separately, the solution for a Gaussian beampattern from a specified piston source with Gaussian apodization was derived by Huang and Breazeale [5], valid within a binomial approximation in cylindrical coordinates as

$$GB[x,z] = \frac{A_0 \exp[Ikz]}{\left(\sigma^2 + \frac{2Iz}{k}\right)} \exp\left[\frac{-x^2}{\left(\sigma^2 + \frac{2Iz}{k}\right)}\right], \tag{6}$$

where σ is the beamwidth at the source, I is the imaginary unit, and A_0 is an amplitude term.

Thus, a Gaussian piston source at the origin produces a Gaussian-shaped beampattern that expands gradually in a lateral direction with increasing range, as expected from general considerations of Fourier acoustics [21].

3. Results

Assuming we have a circular piston source with specified excitation or source function at $\theta = \pi/2$, we find that there are several ways of configuring the weights and spherical Bessel functions so as to produce a close approximation to the Breazeale Gaussian beam. First, by identifying $f(x)$ in Equation (5) as a Gaussian function and $f(n)$ as discrete samples, we make use of the interpolation property along the radial direction. We also introduce a rotating phase on I^n to compensate for the modulo 4 phase relations of the spherical Bessel functions with increasing n [16], and then we can construct

$$BY[x,z] = \sum_{n=0}^{120} I^n (n + 1/2)^{1/2} \exp\left[\frac{-n^2}{(2 \cdot 40^2)}\right] \cdot j_n\left[\left(\frac{2\pi}{0.3}\right)\left(\sqrt{x^2+z^2}\right)\right] \cdot Y_n^0[\theta, 0], \tag{7}$$

where $\theta = \arctan[x/z]$. The scale factor on the Gaussian weights and the spherical Bessel function wavenumber k are set assuming a 5 MHz beam in water with $\lambda = 0.3$ mm, a source width, or standard deviation of approximately 2 mm. The resulting beampattern in this and subsequent cases is calculated using Mathematica (version 13, Wolfram Research, Champaign, IL, USA) and is shown in Figure 2, top. With these practical 5 MHz parameters, the beampattern exhibits only a small amount of lateral spreading at 40 mm range (far right).

The second plot, Figure 2, bottom, removes the I^n factor but includes the imaginary offset $z \to z + Iq$, where q is set to 1/3. In this case, the equation can be given as

$$BY4[x,z] = \sum_{n=0}^{120/4} (4n + 1/2)^{1/2} \exp\left[\frac{-(4n)^2}{(2 \cdot 40^2)}\right] \cdot j_{4n}\left[\left(\frac{2\pi}{0.3}\right)\left(\sqrt{x^2 + \left(z + \frac{1}{3}\right)^2}\right)\right] \cdot Y_{4n}^0[\theta, 0], \tag{8}$$

Also, for $BY4$, the summation takes place only for modulo 4 (i.e., 0, 4, 8. . .120) because this matches the coherent modulo 4 behavior of the spherical functions. A lateral cross section at 30 mm range is shown in Figure 3, representing the similarities between the Breazeale Gaussian and the spherical harmonic solutions. We note that despite the imaginary components in the formulas of GB, BY, and $BY4$, all three formulations have real (effectively zero imaginary) amplitudes at the source, $z = 0$.

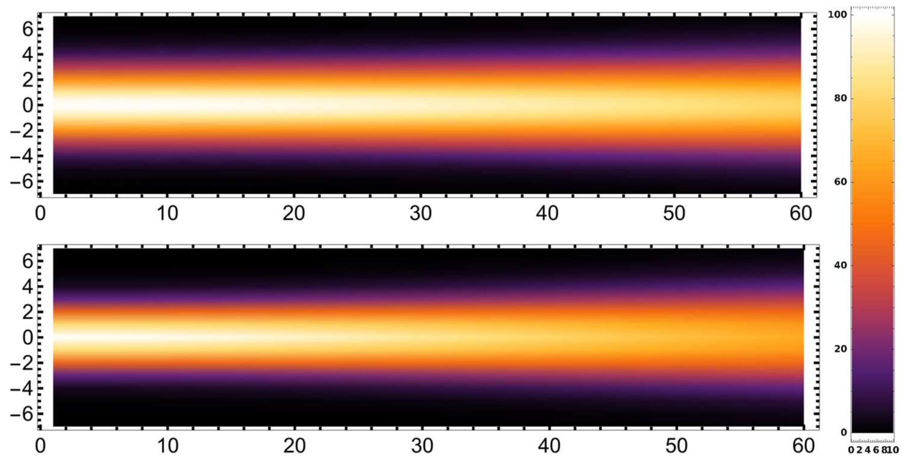

Figure 2. Amplitude plots of 5 MHz fields synthesized from a circularly symmetric source on the left, radiating into free space out to 40 mm on the extreme right, utilizing sums up to integer order 120. The top uses all orders from Equation (7) with a Gaussian weighting function. The bottom uses only every fourth order, with an imaginary offset $q = 1/3$ on the z-coordinate system.

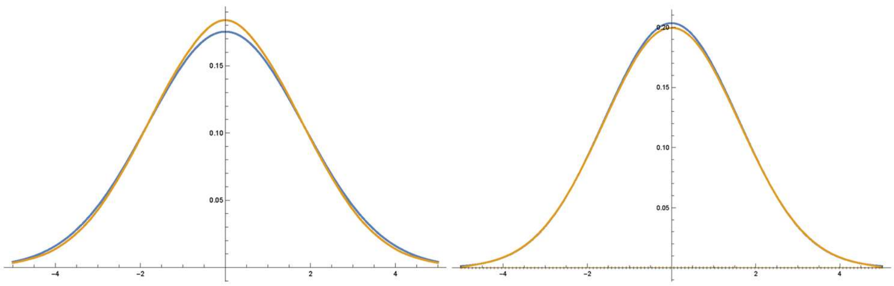

Figure 3. The lateral beamplots for the 5 MHz case of Figure 2, top, and for the Breazeale Gaussian beam (Equation (6) in blue and the BY beam, Equation (7), in yellow, at a 30 mm range (left) and at the source (right), assuming a flat piston source at $\theta = \pi/2$). These are similar functions but are not identical due to differences in formulation: paraxial approximation for the Breazeale Gaussian vs. limited multipoles for the BY beam. The vertical axis is in arbitrary amplitude units; the horizontal axis is in mm.

Turning to broadband pulse examples, we repeat the case of Equation (8) and Figure 2, bottom, with a more broadband pulse centered between 1 and 4 MHz. Following the general definition of a broadband signal from its Fourier transform superposition of different frequencies, we write

$$BY4B[x,z,t] = \int_0^\infty A(\omega)\exp[I\omega t]BY4\left[x,z,\frac{\omega}{c}\right]d\omega. \tag{9}$$

A specific example of this type was calculated using numerical integration (NIntegrate) in Mathematica with

$$A(\omega) = \omega^2 \exp\left[\frac{-\omega^2}{2\pi^4}\right]. \tag{10}$$

This spectral function was chosen for two reasons: it has a practical bandpass shape, and as we show with Parker and Alonso [22], closed-form analytical solutions are available and are compact for the integrand containing products of this type with Bessel functions. The broadband propagation is shown as an intensity plot as a function of time (0–40 μs) in Video S1, and the real part of the pulse is shown in Video S2.

Finally, for cases where the center of the source is reserved for other sensing devices or for cases where the center of the overlying tissue is protected, the convergence of the spherical harmonics is demonstrated from a ring-shaped source. In this case, a Gaussian set of weights a_n are specified by a Gaussian offset, where n^2 in Equation (7) is replaced with $(n-50)^2$, effectively pushing the peak source strength outward from the center. A broadband spectrum centered around 5 MHz is employed, and the convergence of the waveforms toward the axial centerline can be seen in Video S2.

This example demonstrates that a range of customized beampatterns can be constructed using the framework based on the interpolation and localization properties of the sum of the harmonic functions.

4. Discussion and Conclusions

The reconsideration of the classical spherical harmonics solution, along with the recognition of some of the unique properties of these functions, enables the recasting of classical concepts such as apodization and focusing in the design of beampatterns. In the spherical harmonics frame of reference, the specification of the sum of the harmonics with varying weights across a cone or piston source is capable of generating a variety of beams that can be concentrated along the central axis. This includes the classical Gaussian beampattern, which is a useful benchmark function both in experimental work and in theory. We note that the Breazeale Gaussian beampattern from a continuous analytic source function was experimentally realized with a piezoelectric source excited with a similarly shaped voltage. However, the summation formulas of Equations (7) and (8) are compatible with a discrete set of multipoles, as in an array configuration. Thus, these formulations provide an alternative conceptualization and source configuration for the production of Gaussian and other beams. Limitations of this study include the assumption of the high-resolution reproduction of spherical Bessel function waves across the source plane; in reality, the source array elements will have a finite extent, and so the specific measurements of any array configuration would need to be incorporated into a more realistic simulation of the wave propagation into free space. Further research is required to optimize the spatial configuration of source elements and spectral bandwidth for particular uses.

Supplementary Materials: The following supporting information can be downloaded at https://www.mdpi.com/article/10.3390/acoustics7010014/s1; Video S1. The broadband version of $BY4$, which employs a practical bandpass shape with 50% bandwidth from approximately 1 to 4 MHz. The bandpass shape is of the form $(2\pi f)^2 \exp\left[-(2\pi f)^2/(2\pi^4)\right]$, which has favorable properties when combined with Bessel functions in a Fourier transform. The simulation covers 40 µs of propagation over 32 mm of range. The axial range shown is ±5 mm from the center line, and the speed is 1.5 mm/µs. (**a**) The intensity of the complex propagating waveform. This is a ".gif" (15 KB) filetype. (**b**) The real part of the complex waveform, rendered in linear gray scale, with the maximum value saturated white. This is ".gif" (41 KB) filetype; Video S2. A ring-shaped source created by centering Gaussian apodized elements around j_{50} and using the broadband solution. The axial localization property of the superposition of spherical Bessel functions creates a merging zone at an axial distance; no other focusing is employed. A practical bandpass shape centered around 5 MHz. The simulation covers 40 µs of propagation over 40 mm of range. The axial range shown is ±5 mm from the center line, and the speed is 1.5 mm/µs. (**a**) The intensity of the complex propagating waveform. This is a ".gif" (37 KB) filetype. (**b**) The real part of the complex waveform, rendered in linear gray scale, with the maximum value saturated white. This is a ".gif" (105 KB) filetype.

Author Contributions: Conceptualization, K.J.P. and M.A.A.; methodology, K.J.P. and M.A.A.; software, K.J.P. and M.A.A.; writing—original draft preparation, K.J.P.; writing—review and editing, K.J.P. and M.A.A. All authors have read and agreed to the published version of the manuscript.

Funding: This research received no external funding.

Institutional Review Board Statement: Not applicable.

Informed Consent Statement: Not applicable.

Data Availability Statement: The original contributions presented in this study are included in the article/Supplementary Materials. Further inquiries can be directed to the corresponding author.

Acknowledgments: The authors are grateful for continuing support from their respective departments.

Conflicts of Interest: The authors declare no conflicts of interest.

References

1. Goldsmith, P.F. Gaussian beam propagation. In *Quasioptical Systems: Gaussian Beam Quasioptical Propogation and Applications*; IEEE: New York, NY, USA, 1998; pp. 9–38.
2. Bracewell, R.N. *The Fourier Transform and Its Applications*, 1st ed.; McGraw-Hill: New York, NY, USA, 1965.
3. Papoulis, A. *The Fourier Integral and Its Applications*; McGraw-Hill: New York, NY, USA, 1987.
4. Du, G.; Breazeale, M.A. The ultrasonic field of a gaussian transducer. *J. Acoust. Soc. Am.* **1985**, *78*, 2083–2086. [CrossRef]
5. Huang, D.; Breazeale, M.A. An ultrasonic Gaussian transducer and its diffraction field: Theory and practice. *IEEE Trans. Ultrason. Ferroelectr. Freq. Control* **2006**, *53*, 1018–1027. [CrossRef] [PubMed]
6. Moore, N.J.; Alonso, M.A. Closed form formula for Mie scattering of nonparaxial analogues of Gaussian beams. *Opt. Express* **2008**, *16*, 5926–5933. [CrossRef] [PubMed]
7. Moore, N.J.; Alonso, M.A. Mie scattering of highly focused, scalar fields: An analytic approach. *J. Opt. Soc. Am. A Opt. Image Sci. Vis.* **2016**, *33*, 1236–1243. [CrossRef] [PubMed]
8. Gutiérrez-Cuevas, R.; Moore, N.J.; Alonso, M.A. Lorenz-Mie scattering of focused light via complex focus fields: An analytic treatment. *Phys. Rev. A* **2018**, *97*, 053848. [CrossRef]
9. Alonso, M.A.; Moore, N.J. Basis expansions for monochromatic field propagation in free space. In *Mathematical Optics: Classical, Quantum, and Computational Methods*; Lakshminarayanan, V., Calvo, M.L., Alieva., T., Eds.; CRC Press: Boca Raton, Fl, USA, 2013; pp. 98–141.
10. Kravtsov, Y.A. Complex rays and complex caustics. *Radiophys. Quantum El* **1967**, *10*, 719–730. [CrossRef]
11. Deschamps, G.A. Gaussian beam as a bundle of complex rays. *Electron. Lett.* **1971**, *7*, 684–685. [CrossRef]
12. Felsen, L.B. Evanescent waves. *J. Opt. Soc. Am.* **1976**, *66*, 751–760. [CrossRef]
13. Cullen, A.L.; Yu, P.K. Complex source-point theory of the electromagnetic open resonator. *P. Roy. Soc. Lond. A Mat.* **1979**, *366*, 155–171. [CrossRef]
14. Lindell, I.V. Exact-image method for gaussian-beam problems involving a planar interface. *J. Opt. Soc. Am. A* **1987**, *4*, 2185–2190. [CrossRef]
15. Parker, K.J.; Alonso, M.A. The spherical harmonic family of beampatterns. *Acoustics* **2022**, *4*, 958–966. [CrossRef]
16. Abramowitz, M.; Stegun, I.A. *Handbook of Mathematical Functions with Formulas, Graphs, and Mathematical Tables*; U.S. Govt. Print. Off.: Washington, DC, USA, 1964.
17. Kaplan, W. Fourier-Bessel series. In *Advanced Calculus*, 4th ed.; Addison-Wesley: Reading, MA, USA, 1992; pp. 512–518.
18. Stevenson, G. Expansions of the Neumann type in terms of products of Bessel functions. *Am. J. Math.* **1928**, *50*, 569–590. [CrossRef]
19. Watson, G.N. Chapter 16. In *A Treatise on the Theory of Bessel Functions*, 2nd ed.; Cambridge University Press: London, UK, 1944.
20. Erdélyi, A.; Magnus, W.; Oberhettinger, F.; Tricomi, F.G. *Higher Transcendental Functions/Vol. 1*; McGraw-Hill: New York, NY, USA; London, UK, 1953.
21. Williams, E.G. *Fourier Acoustics: Sound Radiation and Nearfield Acoustical Holography*; Academic Press: San Diego, CA, USA, 1999.
22. Parker, K.J.; Alonso, M.A. The Concentrated Toroidal Wave. *arXiv* **2024**, arXiv:2410.11700.